OPO OPHTHALMIC & PHYSIOLOGICAL OPTICS
THE JOURNAL OF THE COLLEGE OF OPTOMETRISTS

Ophthalmic & Physiological Optics ISSN 0275-5408

INVITED REVIEW

Corneal biomechanics – a review

Sabine Kling[1] and Farhad Hafezi[1,2,3,4]

[1]CABMM, University of Zurich, Zurich, Switzerland, [2]ELZA Institute AG Dietikon, Zurich, Switzerland, [3]USC Roski Eye Institute – Keck School of Medicine, Los Angeles, USA, and [4]Ophthalmology, University of Geneva, Geneva, Switzerland

Citation information: Kling S & Hafezi F. Corneal biomechanics – a review. *Ophthalmic Physiol Opt* 2017. doi: 10.1111/opo.12345

Keywords: corneal biomechanics, corneal ectasia, extracellular matrix, numerical simulation

Correspondence: Sabine Kling
E-mail address: kling.sabine@gmail.com

Received: 11 October 2016; Accepted: 15 November 2016

Abstract

Purpose: In recent years, the interest in corneal biomechanics has strongly increased. The material properties of the cornea determine its shape and therefore play an important role in corneal ectasia and related pathologies. This review addresses the molecular origin of biomechanical properties, models for their description, methods for their characterisation, techniques for their modification, and computational simulation approaches.

Recent findings: Recent research has focused on developing non-contact techniques to measure the biomechanical properties *in vivo*, on determining structural and molecular abnormalities in pathological corneas, on developing and optimising techniques to reinforce the corneal tissue and on the computational simulation of surgical interventions.

Summary: A better understanding of corneal biomechanics will help to improve current refractive surgeries, allow an earlier diagnosis of ectatic disorders and a better quantification of treatments aiming at reinforcing the corneal tissue.

Introduction

The corneal shape is a determinant of ocular refraction, but is itself determined by its biomechanical properties. The cornea needs to be soft enough to bulge out in an aspheric half-sphere, but stiff enough to maintain its shape and resist the intraocular pressure (IOP). At the same time, the tissue needs to remain transparent, which requires a complex interplay between the extracellular matrix (ECM) components. Particularly, the attachment of proteoglycans and glycosaminoglycans to collagen fibres, the organisation of the collagen structure, the corneal swelling pressure and the production/degradation of ECM components have been identified as essential factors determining the material properties of the corneal tissue.

Factors determining corneal biomechanical properties

Extracellular matrix (ECM) components

Glycosaminoglycans (GAGs) and proteoglycans (PGs) play an essential role in the assembly of the ECM and its transparency. It is generally understood that keratan sulfate proteoglycans regulate the diameter of collagen fibrils, while dermatan sulfate proteoglycans determine the interfibrillar spacing and lamellar adhesion properties.[1] GAGs interfere with collagen electrostatically only[2] and therefore hardly affect nucleation or growth, but GAGs are required to sulfate PG core proteins. It has been suggested[3] that particularly de-glycosylated small leucine-rich repeat proteoglycan core proteins may modulate the collagen fibrillogenesis and could play a role in several corneal ectatic disorders: in keratoconus, pellucid marginal degeneration and macular corneal dystrophy the amount of highly sulfated keratan sulfate proteoglycans is reduced[4] or absent, respectively.[4] Also, keratoconic corneas show a reduced amount of highly sulfated chondroitin sulfate proteoglycans (CS-PGs) and an increased ratio of glucosaminoglycans: galactosaminoglycans.[5] The amount of acidic GAGs directly correlates with the degree of collagen fibre organisation along the human corneal stroma.[5,6]

Differences in GAG and PG composition are concomitant with physiological modifications.[7] The proportions of GAGs and PGs are strongly dependent on the amount

of available oxygen. Studies on cornea and cartilage conclude that KS, rather than CS, is produced in conditions of O_2 deficiency.[8] This may explain why KS dominates in the posterior stroma.[9] Also, in large animals with high corneal thicknesses – such as cows, pigs or humans – the KS-GAG proportion reaches up to 60–70%,[9] while in small animals, such as mice, KS is completely absent. Also, environmental modifications – such as the wear of contact lenses – have the potential to increase the proportion of keratan sulfate proteoglycans at the cost of chondroitin sulfate proteoglycans. Keratan sulfate proteoglycans are generally understood to stabilise collagen fibrils on the short-range, while chondroitin sulfate/dermatan sulfate proteoglycans stabilize several fibrils as far as lamellae.[10] Therefore, a decrease in chondroitin sulfate proteoglycans potentially weakens the cornea and facilitates the development of corneal ectasia.

Collagen lamellae organisation

Collagen fibril orientation determines corneal transparency, as well as direction-dependent material properties, and correlates with visual acuity across species.[11] Crystallography studies in *ex vivo* tissue show that the human collagen fibres are orthogonally oriented in the centre and circumferentially towards the limbus.[12] Orthogonal orientation provides the highest visual acuity and is expected to best maintain the corneal shape, followed by vertical orientation (marmoset, horse, cow) before circumferential orientation (pig, rabbit mouse). It has been suggested that differences in the stromal collagen arrangement may result from species-specific eye movements, which activate the extraocular rectus muscles in a certain way and evoke counteracting forces to which the collagen fibres align.[11]

In the human cornea, the fibres are more densely packed in the peripupillary cornea.[13] Also, non-linear optical microscopy found a stronger interweaving and steeper angles of the collagen fibres in the anterior than in the posterior cornea,[14] which correlates with an increased shear stress in the anterior cornea when compared to the posterior cornea.[15] Collagen organisation is disturbed in certain degrading pathologies such as keratoconus,[16] demonstrating their importance for maintaining corneal shape.

Hydration/osmotic pressure

The degree of corneal hydration not only affects its transparency, but also its elastic modulus: the more hydrated the corneal tissue, the lower its elastic modulus,[17,18] which potentially arises from an altered collagen attachment to the proteoglycans an/or glycosaminoglycans based on their ionic interaction. The swelling properties of the corneal tissue are not purely osmotic pressure driven, but also arise from electrolyte exclusion due to the collagen fibril volume.[19] At 666 μm thickness, porcine corneas show a hydration of 3.36 $mg_{H_2O}/mg_{dry\_weight}$ and a swelling pressure of 52 mmHg.[20]

Corneal layers and their importance for biomechanical properties

Due to the different collagen orientation and density, each corneal layer contributes to a greater or lesser extent to the overall biomechanical resistance. The epithelium and endothelium as pure cell layers do not directly contribute to corneal stiffness. Elsheikh *et al*[21] showed in human donor eyes that the contribution of the epithelium to corneal stiffness is much lower than that of the stroma and therefore can most likely be neglected. These cell layers may, however, indirectly affect corneal stiffness by regulating its hydration. In Bowman's membrane, the collagen lamellae are most densely packed, and it is considered to be of major importance for corneal stability after laser ablative surgery.[22] The stroma represents the largest part of the cornea and is therefore the layer mainly defining the biomechanical properties of the cornea. In studies where the cornea has been assumed a non-layered material, these typically refer to the stroma. The pre-descemet membrane, also known as Dua's layer, has been discovered only recently.[23] Due to its mechanical strength, it is has been postulated to contribute significantly to corneal stiffness. Yet, more scientific evidence is required.

Diseases associated to corneal biomechanical properties

Several systemic diseases are known to alter the corneal stiffness. Diabetic mellitus patients have a higher corneal resistance factor as measured by the ocular response analyser.[24,25] Also, diabetes has a protective effect on the incidence rate[26] and severity[27] of degrading corneal diseases such as keratoconus. It is assumed that the presence of advanced glycation end products[28] in diabetic corneas leads to an increased non-enzymatic cross-linking of the corneal tissue that provides additional stiffness.

In contrast, the ECM of the keratoconic cornea is disproportionally degraded leading to a loss of collagen fibril orientation,[16] biomechanical weakening[29–32] and out-bulging of the cornea into a conical shape. A susceptibility to keratoconus has been reported with Trisomy 21, Leber's congential amaurosis, Ehler-Danlos syndrome and osteogenesis imperfecta.[33] The latter two diseases directly affect collagen synthesis, and the corneal ectasia potentially arises from an instable collagen network. In Trisomy 21 and Leber's congenital amaurosis, the origin of corneal degradation however is still unclear. Several studies have suggested that both genetic predisposition and environmental factors are required for the manifestation of keratoconus.

Hormonal fluctuations

Changes in corneal stiffness have also been associated with hormonal fluctuations: Increased oestrogen levels during the menstrual cycle correlated with an increase in corneal thickness,[34] a decrease in corneal hysteresis and a decrease in the corneal resistance factor[35] as measured with the ocular response analyser. Also, pregnancy[36–38] and pathologically-reduced levels of thyroid hormones[39] have been reported in context with the onset or progression of corneal ectasia. Oestrogen administration to *ex vivo* corneas reduces the biomechanical stiffness by 36%.[40]

Environmental factors

Little is known on the influence of environmental effects on corneal biomechanics. While eye-rubbing has been associated to keratoconus,[41,42] ageing[43,44] and smoking[45,46] have both been reported to stiffen the corneal tissue and to reduce the incidence of keratoconus.[45] Eye-rubbing induces ocular trauma and may trigger inflammation increasing the degradation of the ECM. In contrast, ageing leads to the accumulation of glycation end products and cigarette smoke contains aldehydes, which both induce non-enzymatic cross-links between collagen molecules providing additional stiffness.[47]

Mechanical description of corneal properties

Similar to most biological tissues, the cornea has viscoelastic properties. Here, elasticity refers to the static properties of a material and arises from the tensile characteristics of the collagen microstructure. Viscosity refers to the dynamic (i.e. time-dependent) properties and arises from the non-covalent rearrangements of the ECM, such as from water diffusion and electrostatic interactions between GAGs and collagen.

Elastic properties

Elastic properties describe the immediate deformation response to the application of a mechanical stress and mainly result from the collagen fibres. When applying a load on the non pre-stressed corneal tissue, in the beginning the collagen fibres are crimped resulting in a toe region in the stress-strain diagram,[48] see *Figure 1a*. Only when the fibres become straight, the tissue deforms

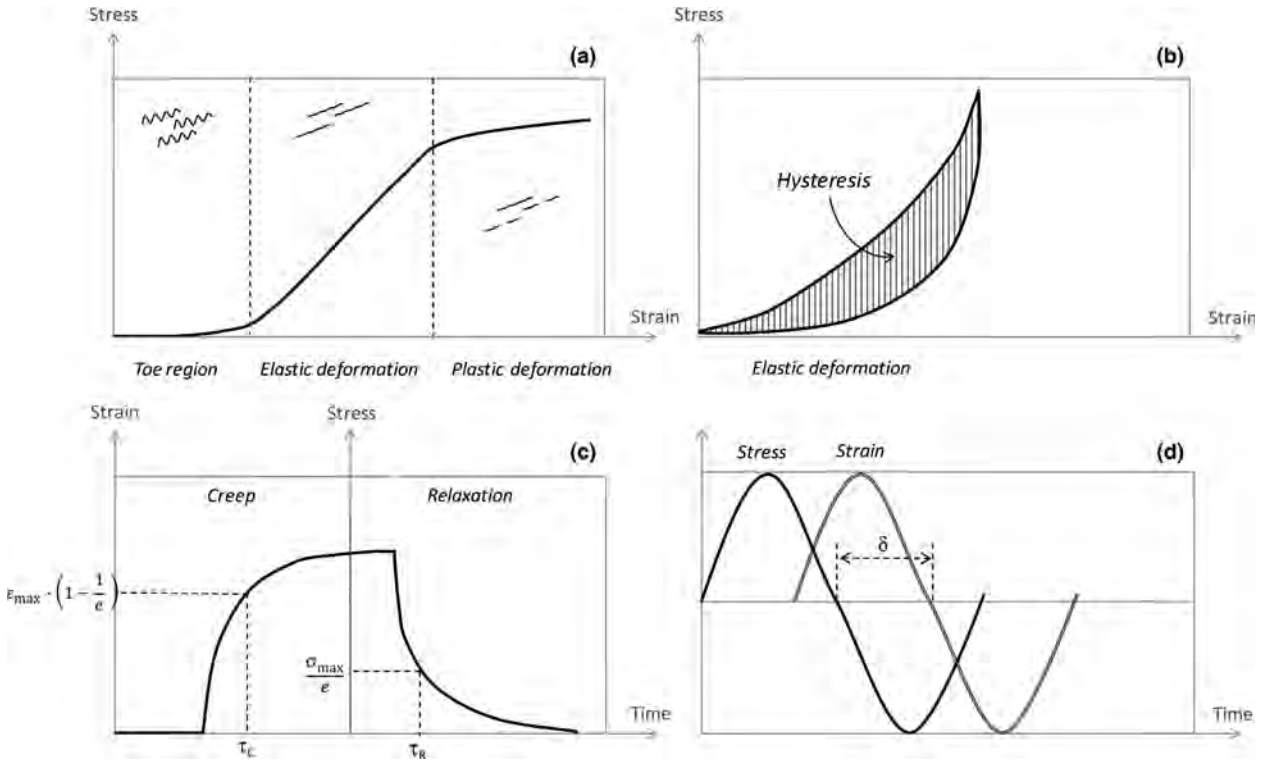

Figure 1. (a) Stress-strain curve for an elastic material. (b) Stress-strain curve for a viscoelastic material. (c) Creep and stress-relaxation in a viscoelastic material. (d) Phase lag between stress and strain in a viscoelastic material.

elastically. It is assumed that the physiological state lies between the end of the toe region and the beginning of the elastic region. When a higher load is applied and the elastic region surpassed, permanent plastic deformation occurs and finally the tissue ruptures.

The standard elastic parameter is the static elastic modulus, also known as Young's modulus. It is defined as the slope of the tangent in the stress-strain diagram.

$$E = \frac{\Delta\sigma}{\Delta\varepsilon} \quad (1)$$

Linear elastic materials have a constant elastic modulus, while in non-linear elastic materials – such as the cornea – the elastic modulus is a function of strain. However, for very small deformation, even non-linear elastic materials deform linearly. Measurements of the corneal elastic modulus range from 1.3 MPa[49] – 5 MPa[50,51] in humans and from 1.5 MPa[49] – 3 MPa[52] in pigs.

Viscoelastic properties

Viscoelastic material properties describe the dynamic deformation response. Time-dependent tissue properties arise from molecular rearrangement, but also from osmotic diffusion as a response to the application of a mechanical load. Viscoelastic deformation is completely reversible with time. In the stress-strain diagram a hysteresis (*Figure 1b*) is observed between the loading and unloading cycle, whose area represents the energy lost during the viscous deformation (e.g. heat).

One possibility to define viscoelastic properties is to use the dynamic modulus, which is composed of the loss and storage modulus. The dynamic modulus E* is based on the fact that stress and strain are out of phase in a viscoelastic material, see *Figure 1d*. Therefore testing at different frequencies is required. The storage (elastic) modulus E' and the loss (viscous) modulus E'' are then defined by the phase lag δ between stress σ and strain ε:

$$E' = \frac{\sigma_o}{\varepsilon_o}. \cos\delta \quad (2a)$$

$$E'' = \frac{\sigma_o}{\varepsilon_o}. \sin\delta \quad (2b)$$

The dynamic modulus can then be calculated by: $E^* = E' + i \cdot E''$ This kind of viscoelastic characterisation demonstrated that in porcine corneas the storage modulus (2–8 kPa) was dominant over the loss modulus (0.3–1.2 kPa).[53]

Another possibility to define viscoelastic properties is to use an *n*-element Prony series. Typically, stress-relaxation test are performed and the stress is fitted to the following equation:

$$\sigma(t) = \sigma_\infty + \sum_{i=1}^{n} \sigma_i \cdot e^{-\frac{t}{\tau_i}} \quad (3)$$

where σ_∞ is the infinite stress and σ_i the stress at a given time point τ_i. Given that the strain ε_0 is maintained constant during stress-relaxation, the elastic moduli at a given time point t can be easily calculated by dividing $\sigma(t)$ by ε_0. See also *Figure 1c*. This kind of viscoelastic definition has been applied in a study to retrieve biomechanical parameters from air-puff deformation.[54]

Measuring corneal biomechanical properties

Table 1 summarises previously applied techniques to measure the biomechanical properties of the cornea.

Extensometry

Stress-strain extensometry is the gold standard method in engineering to measure the macroscopic mechanical properties within a normalized setting. Tissue samples of a predefined length and width are fixed within brackets. Then, a pre-defined load is applied and the corresponding displacement measured. For elastic testing, a slowly increasing load is applied (stress-strain diagram).[49] For viscoelastic testing, a one-step load is applied and maintained constant until the end of the test (stress-relaxation test), or a one-step displacement is applied and maintained constant (creep test).

Given that this kind of extensometry cannot be applied *in vivo* nor in intact *ex vivo* eyes, modifications of the testing procedure have been proposed. For *ex vivo* measurements, corneal button and whole eye inflation set ups were designed, where either the displacement of mercury droplets,[55] graphite flakes,[56] the corneal apex[57] or curvature changes[58] were recorded. For *in vivo* measurements, Pallikaris *et al.*[59] developed a protocol, where the whole eye is inflated during surgery and the corresponding rise in IOP measured in order to determine ocular rigidity. Lam *et al.*[60] used a flat surface cylinder to perform indentation measurements and estimated corneal stiffness from the inward displacement. A problem inherent to whole eye globe measurements is that the corneal deformation cannot be separated from scleral deformation and the average macroscopic corneal stiffness can only be roughly estimated.

Brillouin microscopy

Brillouin microscopy offers the possibility to record a spatially resolved map of corneal stiffness. The macromolecular, quasi-static non-contact measurement is based on

Table 1. Summary of measurement techniques applied to determine the biomechanical properties of the corneal tissue

	Static	Dynamic	Invasive	*Ex vivo*	*In vivo*	Macroscopic	Microscopic
Strip extensometry	Yes	Yes	Yes	Yes[49]	–	Yes	–
Eye inflation	Yes	Yes	Yes	Yes[55–58]	Yes[59]	Yes	–
Brillouin microscopy	–	Yes	–	Yes[64,65]	Yes[63]	–	Yes
Air-puff systems	–	Yes	Minimally	Yes[70]	Yes[74]	Yes	–
Ultrasound elastography	–	Yes	Minimally	Yes[51,80,81]	Yes	–	Yes
OCT elastography	–	Yes	Minimally	Yes[85,86]	Potentially	–	Yes
Enzymatic digestion	Yes	–	Yes	Yes[87–89]	–	Yes	–

Brillouin scattering, which arises from a non-linear interaction between an optical and acoustic wave, in which the material is compressed by the electromagnetic field. The resulting density variation has the effect of an index grating that partially reflects the incident light. By measuring the frequency shift of the backscattered light, information about the mechanical properties of the material can be obtained:

$$M' = \frac{\rho \ \lambda^2 \ \Omega^2}{4n^2}$$

$$M'' = \frac{\rho \ \lambda^2 \ \Omega^2 \ \Delta\Omega^2}{4n^2}$$

where M' is the elastic modulus, M'' is the viscous modulus, ρ is the mass density, λ is the optical wavelength, Ω is the frequency shift $\Delta\Omega$ is the line width and n is the refractive index. The viscoelastic modulus is defined as $M^* = M' + i \ M''$, analogous to the dynamic elastic modulus E^*. Nevertheless, it is unknown how the Brillouin modulus compares to the static elastic modulus.

Although Brillouin scattering has been known since the 1920s[61] until recently only single-point measurements were possible. In 2008, Scarcelli *et al.*[62] presented the first scanning system that allowed to measure the cross-section of intraocular and crystalline lenses. Meanwhile, Brillouin microscopy has also been applied to perform measurements in human eyes *in vivo*,[63] to quantify the stiffening effect of cross-linking[64] and to identify weakened regions in keratoconus corneas.[65] The Brillouin modulus M' of an untreated porcine cornea roughly falls between 2.75 and 2.5 GPa (anterior and posterior) and increases to 2.95 and 2.5 GPa after CXL treatment.[64]

Air-puff tonometry and related systems

Initially, air-puff tonometers have been developed to measure the intraocular pressure (IOP) by non-contact.[66] The required air pressure to applanate the corneal curvature was considered to be equivalent to the IOP. The ocular response analyser[67] was the first device that tried to related the dynamic deformation response of the cornea with biomechanical parameters.[68] It measures the pressure difference between the inward and outward applanation, the so-called corneal hysteresis. The higher the pressure for the inward and the lower the pressure for the outward applanation, the higher is the viscous component. More recently, air-puff tonometry was combined with high-speed Scheimpflug[69–71] and OCT imaging,[72,73] which allowed for the first time to capture both the complete temporal and spatial deformation profile of the cornea during the air-puff event.

While both systems are available for clinical use,[74] the measured parameters are only geometrical and not directly related to actual biomechanical parameters. Nevertheless, several simulations have been suggested to extract biomechanically relevant parameters from these measurements.[54,75,76] Air-puff systems have been used to analyse differences between hyperopia and myopia,[77] between keratoconic and normal corneas[30,32,78] and in corneas with induced swelling.[79] However in most studies only minor to no changes could be detected demonstrating the need of a more detailed analysis of the recorded deformation profile.

Elastography

Conventional ultrasound-based elastography is frequently used in medicine for the diagnosis of pathologies related to the viscoelastic material properties of tissue, such as breast cancer or liver fibrosis. For ophthalmic applications,[51,80,81] ultrafast echo-graphic imaging is required due to the finer structure of the eye and in order to allow high-resolution acquisition.[82] For the measurement of the corneal tissue, contact with a coupling liquid is needed. Ultrasonic shear waves of 15 MHz are typically used to induce microscopic strains in the tissue. The resulting shear wave is then directly recorded by ultrasonic imaging. In large organs where boundary conditions are negligible, the elastic modulus E can be calculated by:

$$E = 3 \ \rho \ c_s^2$$

where c_s is the propagation speed of the induced shear waves and ρ the density of approx. 1000 kg m^{-3}. In the

cornea however the situation is more complex, as strong reflections and mode conversions occur at the interfaces (interiorly the aqueous humour, exteriorly the coupling liquid).[82] The phase velocity $c(w)$ in this context may be approximated by a leaky Lamb wave:

$$c(w) = \sqrt{\frac{w \ th \ c_s}{2\sqrt{3}}}$$

where w is the angular frequency and th the local thickness of the cornea. Corneal elasticity measured by this technique is in the range of 50–190 kPa[82,83] for normal IOP and increases to 890 kPa after CXL.[82] The drawback of ultrasound-based elastography is that contact is required making it uncomfortable for the patient.

Therefore, more recently, non-contact elastography based on OCT imaging has been developed.[84] Because light has less impact on the corneal tissue than ultrasound, low-amplitude elastics waves need to be induced using a different source. The most recent research has applied a micro air-pulse[85,86] for the induction of low-amplitude (<1 μm) elastic waves. The elastic moduli determined by optical coherence elastography are in the range of 60 kPa for untreated porcine corneal samples.[86]

Enzymatic digestion

Although not a direct measure of corneal stiffness, enzymes that degrade the ECM affect the biomechanical properties. Therefore, the speed of digestion of a corneal sample can be used to infer the original stage of cross-linking and estimate corneal stiffness. Depending on the enzyme, certain chemical bonds will be degraded more efficiently than others. Pepsin is a rather unspecific enzyme and degrades many ECM components equally, which often makes it the enzyme of choice for corneal digestion.[87–89] Other enzymes that have been applied in this context are collagenases and trypsin.[87] Although using selective enzymatic digestion would allow studying the impact of certain ECM components on the resulting biomechanical properties, these studies are still outstanding.

Clinical relevance of corneal biomechanics

Corneal stability after laser refractive surgery

Laser ablation has a considerable effect on the biomechanical equilibrium of the cornea. The thinner the stromal bed after surgery, the less tissue can resist the IOP and the higher is the risk of the so-called postoperative ectasia.[90] Although eyes with an undiagnosed pre-operative ectatic disorder are at the highest risk of developing postoperative ectasia, healthy eyes are at risk if too much corneal tissue is ablated or a thick flap is created.[91] It is difficult to predict the maximal amount of corneal ablation necessary to prevent postoperative ectasia for a given patient, as corneal stiffness and thickness vary between individuals. Currently, general safety limits such as a minimal required stromal bed of 250 μm[92] are applied, but still cannot completely prevent keratectasia.[93] However, the remaining risk might potentially be reduced by combining laser ablation surgery with CXL treatment.[94,95] Apart from corneal thickness, the post-surgical refractive stability depends on the wound healing process, and on the time-dependent relaxation behaviour of the viscoelastic cornea.[22,96] Nevertheless, it has been shown that the largest post-surgical change in biomechanical parameters occurs within 1 week after surgery.[97]

Orthokeratology

Instead of direct refractive correction, the objective of orthokeratology contact lenses (OK) is to induce a temporary shape change of the cornea, so that by day corneal refraction is corrected, while by night,the OK is worn. OK have a reversed geometry compared to normal contact lenses. The working principle is based on the viscoelastic properties of the corneal tissue, which allow maintaining a deformation for limited time. However, rather than corneal bending, a thinning of the central epithelium and a thickening of the mid-peripheral corneal stroma were observed with OK wear.[98] It can be assumed that the pressure imposed by the OK induces an osmotic gradient that removes liquid from the central epithelium. Due to individual differences in the corneal viscoelasticity however, OK lenses are more challenging to fit than standard contact lenses.[99]

Corneal thickness and biomechanical properties

Corneal thickness and biomechanical properties are closely related. On one hand, biomechanical properties determine the extension of the corneal tissue under the load of the IOP, which indirectly determines corneal thickness. On the other hand, a thicker cornea can better resist the load of the IOP than a thinner one and therefore can partially compensate for a low biomechanical stiffness. Corneal thickness plays an essential role in measurements depending on corneal deformation, such as in tonometry.

Intraocular pressure and biomechanical properties

An accurate measurement of the intraocular pressure (IOP) is essential in the diagnosis of glaucoma.[100] Due to limited accessibility of the posterior chamber, the IOP is typically measured via the cornea. While different contact and

non-contact systems exist, the obtained IOP values are biased by the corneal thickness and its biomechanical properties: The thinner and the weaker the cornea, the lower the value obtained. This constitutes an important problem in the diagnosis of glaucoma, especially in patients after laser refractive surgery. While nomograms have been developed to correct the IOP reading for corneal thickness, the correction for corneal biomechanics is more complicated and is currently not possible. In addition, corneal curvature also has an impact on tonometric measurements.[101] The dependency on many factors may explain why air-puff measurements have a low sensitivity and specificity to detect a difference between thin and keratoconic corneas.[78]

Reinforcing corneal biomechanical properties

Corneal cross-linking (CXL) treatment

Corneal cross-linking[102,103] is a photodynamic method that is based on the generation of oxygen radicals by means of riboflavin and UV-A irradiation. While the interaction of the oxygen radicals with the cornea tissue is not yet completely understood, ECM oxidation potentially leads to the formation of additional cross-links. Experimental studies[49,58,83,104] report that corneal stiffness significantly increased after CXL and clinical studies[105,106] could demonstrate that the progression of keratoconus could be stopped. CXL treatment induces keratocyte apoptosis in the anterior cornea. Therefore, current endothelial safety considerations restrict the treatment to corneal thicknesses of >400 μm with the current irradiation settings used in clinical practice.[107] One to two weeks post surgery a demarcation line can be observed in a depth of approximately 300 μm,[108] which potentially arises from a change in the refractive index and may indicate the zone of effective corneal stiffening.[105] CXL has been shown to stabilise corneal ectasia on the long-term.[106] In an *ex vivo* study,[49] corneal stiffness increased by 329% in human and by 72% in porcine corneas after CXL treatment.

Proteoglycan treatment

Proteoglycans are an essential requisite for the interaction and mutual binding of ECM components. Decorin is an important regulatory element of the collagen fibril assembly. Studies on decorin-null mice presented a disrupted collagen fibril structure and organisation especially in the posterior cornea.[109] Crystallography analysis of corneal samples with a truncated decorin mutation confirmed this finding.[110] The administration of decorin core protein to a keratoconic cornea therefore might have the potential to re-establish the physiologic collagen structure and halt the progressing ectasia. A recent experimental study showed that decorin application induced a stiffening of 92% in porcine eyes.[111] Compared to CXL with a 72% stiffening in porcine eyes,[49] decorin core treatment does not require de-epithelialisation nor UV irradiation and therefore might be less invasive. It is yet however unclear how long the stiffening effect will last and if the same results can be obtained *in vivo*.

SMILE lenticule implantation

SMILE lenticule implantation aims at correcting hyperopia. It requires a donor lenticule from a patient undergoing a high-dioptre myopic SMILE surgery, which subsequently is implanted in the previously created corneal pocket of the recipient eye. The central tissue addition allows then to correct the refraction.[112,113] While the primary objective of this surgery is clearly refractive, adding tissue locally also has a biomechanical effect: An increased corneal thickness reduces the longitudinal stress, which in turn leads to a flattening of the corneal curvature. This unintended flattening acts contrary to the desired central steepening, and might explain why only 50% of the expected refractive correction were achieved after SMILE lenticule implantation.[112]

Animal models for corneal biomechanics

Most species present a lower corneal stiffness and a higher viscoelastic creep behaviour than humans, which might be attributed to differences in the fibrillar collagen arrangement.[11]

For *ex vivo* experiments, freshly enucleated porcine corneas are often used[49,58,64,70,87,88,111] because of their similar anatomy compared to the human cornea. In view of anatomical differences only a less developed or absent Bowman's membrane[114–116] and a higher corneal thickness (666 μm centrally)[117] becomes apparent in the porcine cornea. In view of biomechanical properties[52] however, porcine corneas have different stress-relaxation properties and are less stiff than human corneas.[118,119] Nevertheless – considering their abundant availability – porcine eyes are widely accepted as a model for biomechanical studies of the cornea.

For *in vivo* studies, rabbit corneas are widely used due to their large corneas – with a diameter of 13.2 mm and a corneal radius of 7.3 mm.[120] In view of biomechanical properties, at low IOP rabbit corneas deform non-linearly, while human corneas do not deform at all – at higher IOP the stress-strain relation is more similar and linear in both species.[50] Recently, our group has established a corneal biomechanics model in the mouse eye.[121] We observed a linear stress-strain relation similar to rabbit corneas, which could make the mouse an attractive model for studies addressing the molecular origin of biomechanical parameters.

Computational modelling of corneal biomechanics

Before any prediction of reinforcing treatments or refractive surgical interventions can be performed, it is important to construct a representative model of the intact eye. While analytical models are less demanding computationally, they only offer limited flexibility and are not suitable to individual patient modelling. Most biomechanical simulations in ophthalmology therefore use numerical approaches. Depending on the relevant characteristics and the desired degree of accuracy, the model may consider species-specific input data such as collagen fibril orientation[122] and patient-specific[123] topography and pachymetry data. For this purpose, fibril orientation may be defined by using an anisotropic material and corneal elevation coordinates can be directly used to define the nodes of a finite element model. A more difficult issue is to account for the IOP. Typically, the model is defined for the stress-free geometry – which however is unknown for the cornea. To overcome this issue, inverse modelling needs to be performed: Either the IOP-induced stress is computed step-wise until the initial stress state of the cornea is determined,[124] or the provoked deformation is calculated step-wise and subtracted from the stressed geometry in order to obtain the stress-free geometry.[123]

For final validation purposes, the model can be applied to simulate an experiment. For inflation experiments, the comparison of model predictions and experimental measurements could previously confirm a good performance.[125,126]

Corneal ectasia and corneal cross-linking

Numerical simulations might be a helpful tool to predict the individual success rate of CXL in stopping progression of ectasia, but also to predict the associated corneal reshaping and hence refractive changes. Several *in silico* (computational) studies have predicted the weakening profile of a cornea presenting keratectasia[127] and the expected response to CXL treatment.[123,127] These simulations could confirm the clinically observed topographic flattening after CXL,[127] but showed important inter-patient variability indicating the need for patient-specific modeling.[123] In a specific attempt to reduce astigmatism, the simulation of patterned CXL has shown promising effects.[128]

Refractive surgery

One of the major difficulties in refractive surgery is the uncertainty how much tissue can be ablated from a patient's cornea without inducing postoperative ectasia. Several years ago, computer models addressed the potential of myopic and astigmatic correction by incision surgery.[129,130] More recently, simulations are applied to estimate the long-term impact of laser ablative surgery: PRK surgery showed to increase the corneal stress by approx. 25%,[131] while LASIK surgery was predicted to induce a 55% corneal weakening.[132] A comparison between LASIK and SmILE refractive surgery concluded that SmILE increases the corneal stress to a lesser amount than LASIK,[133] which also has been suggested theoretically.[134] Further simulations could show that the refractive outcome after LASIK depends on the inherent corneal stiffness – not only on the amount of tissue ablated,[135] and that tonometry underestimates the actual IOP following PRK or LASIK surgery.[130]

Intra-corneal ring segment (ICRS) implantation

ICRSs serve as a re-shaping and homogenising element in highly distorted corneal surfaces.[136] They are used to improve the visual outcome, but also to make the corneal surface better suited for contact lens wear. The corneal response to ICRS implantation is mostly geometrical and to a minor extent mechanical: The arc length of the cornea is reduced leading to a flatter corneal curvature and a slightly shorter axial length of the eye.[137] The weaker tissue regions will be deformed more strongly. While there are few publications addressing the simulation of ICRS implantation,[136–138] most of them only predict the average response of the cornea and do not allow patient-specific analyses: The thicker the ICRS, the higher the myopic correction. Up to date, only one study presented a patient-specific ICRS model, which however showed a consistent overestimation compared to the actual post-surgical outcome.[139]

Disclosure

SK (none), FH (none).

References

1. Michelacci Y. Collagens and proteoglycans of the corneal extracellular matrix. *Braz J Med Biol Res* 2003; 36: 1037–1046.
2. Scott JE. Proteoglycan-fibrillar collagen interactions. *Biochem J* 1988; 252: 313–323.
3. Kao WW-Y & Liu C-Y. Roles of lumican and keratocan on corneal transparency. *Glycoconjugate J* 2002; 19: 275–285.
4. Funderburgh J, Funderburgh M, Rodrigues M, Krachmer J & Conrad G. Altered antigenicity of keratan sulfate proteoglycan in selected corneal diseases. *Invest Ophthalmol Vis Sci* 1990; 31: 419–428.
5. Praus R & Goldman J. Glycosaminoglycans in human comeal buttons removed at keratoplasty. *Ophthalmic Res* 1971; 2: 223–230.

6. Borcherding MS, Blacik L, Sittig R, Bizzell JW, Breen M & Weinstein H. Proteoglycans and collagen fibre organization in human corneoscleral tissue. *Exp Eye Res* 1975; 21: 59–70.
7. Praus R & Goldman JN. Glycosaminoglycans in the nonswelling corneal stroma of dogfish shark. *Invest Ophthalmol Vis Sci* 1970; 9: 131–136.
8. Scott JE & Haigh M. Keratan sulphate and the ultrastructure of cornea and cartilage: a'stand-in'for chondroitin sulphate in conditions of oxygen lack? *J Anat* 1988; 158: 95–108.
9. Bron A. The architecture of the corneal stroma. *Br J Ophthalmol* 2001; 85: 379–381.
10. Quantock AJ, Young RD & Akama TO. Structural and biochemical aspects of keratan sulphate in the cornea. *Cell Mol Life Sci* 2010; 67: 891–906.
11. Hayes S, Boote C, Lewis J *et al.* Comparative study of fibrillar collagen arrangement in the corneas of primates and other mammals. *Anat Rec* 2007; 290: 1542–1550.
12. Meek KM & Boote C. The use of X-ray scattering techniques to quantify the orientation and distribution of collagen in the corneal stroma. *Prog Retin Eye Res* 2009; 28: 369–392.
13. Boote C, Dennis S, Newton RH, Puri H & Meek KM. Collagen fibrils appear more closely packed in the prepupillary cornea: optical and biomechanical implications. *Invest Ophthalmol Vis Sci* 2003; 44: 2941–2948.
14. Jester JV, Winkler M, Jester BE, Nien C, Chai D & Brown DJ. Evaluating corneal collagen organization using high resolution non linear optical (NLO) macroscopy. *Eye Contact Lens* 2010; 36: 260–264.
15. Petsche SJ, Chernyak D, Martiz J, Levenston ME & Pinsky PM. Depth-dependent transverse shear properties of the human corneal stroma. *Invest Ophthalmol Vis Sci* 2012; 53: 873–880.
16. Meek KM, Tuft SJ, Huang Y *et al.* Changes in collagen orientation and distribution in keratoconus corneas. *Invest Ophthalmol Vis Sci* 2005; 46: 1948–1956.
17. Hatami-Marbini H & Etebu E. Hydration dependent biomechanical properties of the corneal stroma. *Exp Eye Res* 2013; 116: 47–54.
18. Kling S & Marcos S. Effect of hydration state and storage media on corneal biomechanical response from *in vitro* inflation tests. *J Refract Surg* 2013; 29: 490–497.
19. Cheng X, Hatami-Marbini H & Pinsky PM. Modeling collagen-proteoglycan structural interactions in the human cornea. In: *Computer Models in Biomechanics* (Gerhard A. Holzapfel, Ellen Kuhl editors), Springer: Netherlands, 2013; pp. 11–24.
20. Hatami-Marbini H, Etebu E & Rahimi A. Swelling pressure and hydration behavior of porcine corneal stroma. *Curr Eye Res* 2013; 38: 1124–1132.
21. Elsheikh A, Alhasso D & Rama P. Assessment of the epithelium's contribution to corneal biomechanics. *Exp Eye Res* 2008; 86: 445–451.
22. Dawson DG, Grossniklaus HE, Edelhauser HF & McCarey BE. Biomechanical and wound healing characteristics of corneas after excimer laser keratorefractive surgery. *J Refract Surg* 2008; 24: S90–S96.
23. Dua HS, Faraj LA, Said DG, Gray T & Lowe J. Human corneal anatomy redefined: a novel pre-Descemet's layer (Dua's layer). *Ophthalmology* 2013; 120: 1778–1785.
24. Kotecha A, Oddone F, Sinapis C *et al.* Corneal biomechanical characteristics in patients with diabetes mellitus. *J Cataract Refr Surg* 2010; 36: 1822–1828.
25. Krueger RR & Ramos-Esteban JC. How might corneal elasticity help us understand diabetes and intraocular pressure? *J Refract Surg* 2007; 23: 85–88.
26. Seiler T, Huhle S, Spoerl E & Kunath H. Manifest diabetes and keratoconus: a retrospective case-control study. *Graefes Arch Clin Exp Ophthalmol* 2000; 238: 822–825.
27. Kuo IC, Broman A, Pirouzmanesh A & Melia M. Is there an association between diabetes and keratoconus? *Ophthalmology* 2006; 113: 184–190.
28. Kaji Y, Usui T, Oshika T *et al.* Advanced glycation end products in diabetic corneas. *Invest Ophthalmol Vis Sci* 2000; 41: 362–368.
29. Vellara HR & Patel DV. Biomechanical properties of the keratoconic cornea: a review. *Clin Exp Optom* 2015; 98: 31–38.
30. Johnson RD, Nguyen MT, Lee N & Hamilton DR. Corneal biomechanical properties in normal, forme fruste keratoconus, and manifest keratoconus after statistical correction for potentially confounding factors. *Cornea* 2011; 30: 516–523.
31. Fontes BM, Ambrósio R, Jardim D, Velarde GC & Nosé W. Corneal biomechanical metrics and anterior segment parameters in mild keratoconus. *Ophthalmology* 2010; 117: 673–679.
32. Wolffsohn JS, Safeen S, Shah S & Laiquzzaman M. Changes of corneal biomechanics with keratoconus. *Cornea* 2012; 31: 849–854.
33. Kenney MC & Brown DJ. The cascade hypothesis of keratoconus. *Cont Lens Anterior Eye* 2003; 26: 139–146.
34. Kiely PM, Carney LG & Smith G. Menstrual cycle variations of corneal topography and thickness. *Optom Vis Sci* 1983; 60: 822–829.
35. Goldich Y, Barkana Y, Pras E *et al.* Variations in corneal biomechanical parameters and central corneal thickness during the menstrual cycle. *J Cataract Refr Surg* 2011; 37: 1507–1511.
36. Bilgihan K, Hondur A, Sul S & Ozturk S. Pregnancy-induced progression of keratoconus. *Cornea* 2011; 30: 991–994.
37. Hafezi F, Koller T, Derhartunian V & Seiler T. Pregnancy may trigger late onset of keratectasia after LASIK. *J Refract Surg* 2012; 28: 242–243.
38. Padmanabhan P, Radhakrishnan A & Natarajan R. Pregnancy-triggered iatrogenic (post-laser *in situ*

keratomileusis) corneal ectasia—a case report. *Cornea* 2010; 29: 569–572.
39. Gatzioufas Z & Thanos S. Acute keratoconus induced by hypothyroxinemia during pregnancy. *J Endocrinol Invest* 2008; 31: 262–266.
40. Spoerl E, Zubaty V, Raiskup-Wolf F & Pillunat LE. Oestrogen-induced changes in biomechanics in the cornea as a possible reason for keratectasia. *Brit J Ophthalmol* 2007; 91: 1547–1550.
41. Jafri B, Lichter H & Stulting RD. Asymmetric keratoconus attributed to eye rubbing. *Cornea* 2004; 23: 560–564.
42. Bawazeer AM, Hodge WG & Lorimer B. Atopy and keratoconus: a multivariate analysis. *Brit J Ophthalmol* 2000; 84: 834–836.
43. Elsheikh A, Wang D, Brown M, Rama P, Campanelli M & Pye D. Assessment of corneal biomechanical properties and their variation with age. *Curr Eye Res* 2007; 32: 11–19.
44. Cartwright NEK, Tyrer JR & Marshall J. Age-related differences in the elasticity of the human cornea. *Invest Ophthalmol Vis Sci* 2011; 52: 4324–4329.
45. Raiskup-Wolf F, Spoerl E, Kuhlisch E & Pillunat LE. Cigarette smoking is negatively associated with keratoconus. *J Refract Surg* 2008; 24: S737–S740.
46. Hafezi F. Smoking and corneal biomechanics. *Ophthalmology* 2009; 116: 2259–e1.
47. Madhukumar E & Vijayammal P. Influence of cigarette smoke on cross-linking of dermal collagen. *Indian J Exp Biol* 1997; 35: 483–486.
48. Sharma P & Maffulli N. Tendon injury and tendinopathy: healing and repair. *J Bone Joint Surg* 2005; 87: 187–202.
49. Wollensak G, Spoerl E & Seiler T. Stress-strain measurements of human and porcine corneas after riboflavin–ultraviolet-A-induced cross-linking. *J Cataract Refr Surg* 2003; 29: 1780–1785.
50. Jue B & Maurice DM. The mechanical properties of the rabbit and human cornea. *J Biomech* 1986; 19: 847–853.
51. Wang H, Prendiville PL, McDonnell PJ & Chang WV. An ultrasonic technique for the measurement of the elastic moduli of human cornea. *J Biomech* 1996; 29: 1633–1636.
52. Kampmeier J, Radt B, Birngruber R & Brinkmann R. Thermal and biomechanical parameters of porcine cornea. *Cornea* 2000; 19: 355–363.
53. Hatami-Marbini H. Viscoelastic shear properties of the corneal stroma. *J Biomech* 2014; 47: 723–728.
54. Kling S, Bekesi N, Dorronsoro C, Pascual D & Marcos S. Corneal viscoelastic properties from finite-element analysis of *in vivo* air-puff deformation. *PLoS ONE* 2014; 9: e104904.
55. Hjortdal JØ. Regional elastic performance of the human cornea. *J Biomech* 1996; 29: 931–942.
56. Boyce BL, Grazier JM, Jones RE & Nguyen TD. Full-field deformation of bovine cornea under constrained inflation conditions. *Biomaterials* 2008; 29: 3896–3904.
57. Elsheikh A & Anderson K. Comparative study of corneal strip extensometry and inflation tests. *J R Soc Interface* 2005; 2: 177–185.
58. Kling S, Remon L, Pérez-Escudero A, Merayo-Lloves J & Marcos S. Corneal biomechanical changes after collagen cross-linking from porcine eye inflation experiments. *Invest Ophthalmol Vis Sci* 2010; 51: 3961–3968.
59. Pallikaris IG, Kymionis GD, Ginis HS, Kounis GA & Tsilimbaris MK. Ocular rigidity in living human eyes. *Invest Ophthalmol Vis Sci* 2005; 46: 409–414.
60. Lam AK, Hon Y, Leung LK & Lam DC. Repeatability of a novel corneal indentation device for corneal biomechanical measurement. *Ophthalmic Physlio Opt* 2015; 35: 455–461.
61. Brillouin L. Diffusion de la lumière et des rayons X par un corps transparent homogène. Influence de l'agitation thermique. *Ann Phys* 1922; 17: 21.
62. Scarcelli G & Yun SH. Confocal Brillouin microscopy for three-dimensional mechanical imaging. *Nat Photonics* 2008; 2: 39–43.
63. Scarcelli G & Yun SH. *In vivo* Brillouin optical microscopy of the human eye. *Opt Express* 2012; 20: 9197–9202.
64. Scarcelli G, Kling S, Quijano E, Pineda R, Marcos S & Yun SH. Brillouin microscopy of collagen crosslinking: noncontact depth-dependent analysis of corneal elastic modulus. *Invest Ophthalmol Vis Sci* 2013; 54: 1418–1425.
65. Scarcelli G, Besner S, Pineda R & Yun SH. Biomechanical characterization of keratoconus corneas *ex vivo* with brillouin microscopy. *Invest Ophthalmol Vis Sci* 2014; 55: 4490–4495.
66. Forbes M, Pico G & Grolman B. A noncontact applanation tonometer: description and clinical evaluation. *Ama Arch Ophthalmol* 1974; 91: 134–140.
67. Luce DA. Determining *in vivo* biomechanical properties of the cornea with an ocular response analyzer. *J Cataract Refr Surg* 2005; 31: 156–162.
68. Terai N, Raiskup F, Haustein M, Pillunat LE & Spoerl E. Identification of biomechanical properties of the cornea: the ocular response analyzer. *Curr Eye Res* 2012; 37: 553–562.
69. Hon Y & Lam AK. Corneal deformation measurement using Scheimpflug noncontact tonometry. *Optom Vis Sci* 2013; 90: e1–e8.
70. Kling S & Marcos S. Contributing factors to corneal deformation in air puff measurements. *Invest Ophthalmol Vis Sci* 2013; 54: 5078–5085.
71. Ambrósio R Jr, Ramos I, Luz A *et al.* Dynamic ultra high speed Scheimpflug imaging for assessing corneal biomechanical properties. *Rev Bras Oftalmol* 2013; 72: 99–102.
72. Alonso-Caneiro D, Karnowski K, Kaluzny BJ, Kowalczyk A & Wojtkowski M. Assessment of corneal dynamics with high-speed swept source optical coherence tomography combined with an air puff system. *Opt Express* 2011; 19: 14188–14199.

73. Dorronsoro C, Pascual D, Pérez-Merino P, Kling S & Marcos S. Dynamic OCT measurement of corneal deformation by an air puff in normal and cross-linked corneas. *Biomed Opt Express* 2012; 3: 473–487.
74. Piñero DP & Alcón N. *In vivo* characterization of corneal biomechanics. *J Cataract Rerfr Surg* 2014; 40: 870–887.
75. Roy AS, Kurian M, Matalia H & Shetty R. Air-puff associated quantification of non-linear biomechanical properties of the human cornea *in vivo*. *J Mech Behav Biomed* 2015; 48: 173–182.
76. Shih PJ, Cao HJ, Huang CJ, Wang I, Shih WP & Yen JY. A corneal elastic dynamic model derived from Scheimpflug imaging technology. *Ophthalmic Physlio Opt* 2015; 35: 663–672.
77. Qazi MA, Roberts CJ, Mahmoud AM & Pepose JS. Topographic and biomechanical differences between hyperopic and myopic laser *in situ* keratomileusis. *J Cataract Refr Surg* 2005; 31: 48–60.
78. Fontes BM, Ambrósio R Jr, Velarde GC & Nosé W. Corneal biomechanical evaluation in healthy thin corneas compared with matched keratoconus cases. *Arq Bras Oftalmol* 2011; 74: 13–16.
79. Lau W & Pye D. Changes in corneal biomechanics and applanation tonometry with induced corneal swelling. *Invest Ophth Vis Sci* 2011; 52: 3207–3214.
80. He X & Liu J. A quantitative ultrasonic spectroscopy method for noninvasive determination of corneal biomechanical properties. *Invest Ophthalmol Vis Sci* 2009; 50: 5148–5154.
81. Liu J, He X, Pan X & Roberts CJ. Ultrasonic model and system for measurement of corneal biomechanical properties and validation on phantoms. *J Biomech* 2007; 40: 1177–1182.
82. Tanter M, Touboul D, Gennisson J-L, Bercoff J & Fink M. High-resolution quantitative imaging of cornea elasticity using supersonic shear imaging. *IEEE T Med Imaging* 2009; 28: 1881–1893.
83. Touboul D, Gennisson J-L, Nguyen T-M *et al.* Supersonic shear wave elastography for the *in vivo* evaluation of transepithelial corneal collagen cross-linking. *Invest Ophthalmol Vis Sci* 2014; 55: 1976–1984.
84. Wang S & Larin KV. Optical coherence elastography for tissue characterization: a review. *J Biophotonics* 2015; 8: 279–302.
85. Twa MD, Li J, Vantipalli S *et al.* Spatial characterization of corneal biomechanical properties with optical coherence elastography after UV cross-linking. *Biomed Opt Express* 2014; 5: 1419–1427.
86. Han Z, Aglyamov SR, Li J *et al.* Quantitative assessment of corneal viscoelasticity using optical coherence elastography and a modified Rayleigh–Lamb equation. *J Biomed Opt* 2015; 20: 1–3.
87. Spoerl E, Wollensak G & Seiler T. Increased resistance of crosslinked cornea against enzymatic digestion. *Curr Eye Rres* 2004; 29: 35–40.
88. Aldahlawi NH, Hayes S, O'Brart DP, Akhbanbetova A, Littlechild SL & Meek KM. Enzymatic resistance of corneas crosslinked using riboflavin in conjunction with low energy, high energy, and pulsed UVA irradiation modes. *Invest Ophthalmol Vis Sci* 2016; 57: 1547–1552.
89. Aldahlawi NH, Hayes S, O'Brart DP & Meek KM. Standard versus accelerated riboflavin–ultraviolet corneal collagen crosslinking: resistance against enzymatic digestion. *J Cataract Refr Surg* 2015; 41: 1989–1996.
90. Rabinowitz YS. Ectasia after laser *in situ* keratomileusis. *Curr Opin Ophthalmol* 2006; 17: 421–426.
91. Ambrósio R Jr, Nogueira LP, Caldas DL *et al.* Evaluation of corneal shape and biomechanics before LASIK. *Int Ophthalmol Clin* 2011; 51: 11–38.
92. Seiler T, Koufala K & Richter G. Iatrogenic keratectasia after laser *in situ* keratomileusis. *J Refract Surg* 1998; 14: 312–317.
93. Ou RJ, Shaw EL & Glasgow BJ. Keratectasia after laser *in situ* keratomileusis (LASIK): evaluation of the calculated residual stromal bed thickness. *Am J Ophthalmol* 2002; 134: 771–773.
94. Kanellopoulos AJ & Pamel GJ. Review of current indications for combined very high fluence collagen cross-linking and laser *in situ* keratomileusis surgery. *Indian J Ophthalmol* 2013; 61: 430–432.
95. Kling S, Spiru B, Hafezi F & Sekundo W. Biomechanical analysis of different re-treatment options after SmILE refractive surgery. *J Refract Surg* (in press).
96. Dupps WJ & Wilson SE. Biomechanics and wound healing in the cornea. *Exp Eye Res* 2006; 83: 709–720.
97. Kamiya K, Shimizu K & Ohmoto F. Time course of corneal biomechanical parameters after laser *in situ* keratomileusis. *Ophthal Res* 2009; 42: 167–171.
98. Swarbrick HA, Wong G & O'Leary DJ. Corneal response to orthokeratology. *Optom Vis Sci* 1998; 75: 791–799.
99. Binder PS, May CH & Grant SC. An evaluation of orthokeratology. *Ophthalmology* 1980; 87: 729–744.
100. Sultan MB, Mansberger SL & Lee PP. Understanding the importance of IOP variables in glaucoma: a systematic review. *Surf Ophthalmol* 2009; 54: 643–662.
101. Broman AT, Congdon NG, Bandeen-Roche K & Quigley HA. Influence of corneal structure, corneal responsiveness, and other ocular parameters on tonometric measurement of intraocular pressure. *J Glaucoma* 2007; 16: 581–588.
102. Spoerl E, Huhle M & Seiler T. Induction of cross-links in corneal tissue. *Exp Eye Res* 1998; 66: 97–103.
103. Meek KM & Hayes S. Corneal cross-linking–a review. *Ophthalmic Physlio Opt* 2013; 33: 78–93.
104. Aldahlawi NH, Hayes S, O'Brart DP, O'Brart ND & Meek KM. An investigation into corneal enzymatic resistance following epithelium-off and epithelium-on corneal cross-linking protocols. *Experimental Eye Research* 2016; 153: 141–151.
105. Kymionis GD, Tsoulnaras KI, Grentzelos MA *et al.* Evaluation of corneal stromal demarcation line depth following

standard and a modified-accelerated collagen cross-linking protocol. *Am J Ophthalmol* 2014; 158: 671–675 e1.
106. Raiskup-Wolf F, Hoyer A, Spoerl E & Pillunat LE. Collagen crosslinking with riboflavin and ultraviolet-A light in keratoconus: long-term results. *J Cataract Refr Surg* 2008; 34: 796–801.
107. Spoerl E, Mrochen M, Sliney D, Trokel S & Seiler T. Safety of UVA-riboflavin cross-linking of the cornea. *Cornea* 2007; 26: 385–389.
108. Seiler T & Hafezi F. Corneal cross-linking-induced stromal demarcation line. *Cornea* 2006; 25: 1057–1059.
109. Zhang G, Chen S, Goldoni S *et al.* Genetic evidence for the coordinated regulation of collagen fibrillogenesis in the cornea by decorin and biglycan. *J Biol Chem* 2009; 284: 8888–8897.
110. Kamma-Lorger CS, Pinali C, Martínez JC *et al.* Role of decorin core protein in collagen organisation in congenital stromal corneal dystrophy (CSCD). *PLoS ONE* 2016; 11: e0147948.
111. Metzler KM, Roberts CJ, Mahmoud AM, Agarwal G & Liu J. *Ex vivo* transepithelial collagen cross-linking in porcine and human corneas using human decorin core protein. *J Refract Surg* 2016; 32: 410–417.
112. Pradhan KR, Reinstein DZ, Carp GI, Archer TJ, Gobbe M & Gurung R. Femtosecond laser-assisted keyhole endokeratophakia: correction of hyperopia by implantation of an allogeneic lenticule obtained by SMILE from a myopic donor. *J Refract Surg* 2013; 29: 777–782.
113. Ganesh S, Brar S & Rao PA. Cryopreservation of extracted corneal lenticules after small incision lenticule extraction for potential use in human subjects. *Cornea* 2014; 33: 1355–1362.
114. Sanchez I, Martin R, Ussa F & Fernandez-Bueno I. The parameters of the porcine eyeball. *Graefes Arch Clin Exp Ophthalmol* 2011; 249: 475–482.
115. Lai T & Tang S. Cornea characterization using a combined multiphoton microscopy and optical coherence tomography system. *Biomed Opt Express* 2014; 5: 1494–1511.
116. Jay L, Brocas A, Singh K, Kieffer J-C, Brunette I & Ozaki T. Determination of porcine corneal layers with high spatial resolution by simultaneous second and third harmonic generation microscopy. *Opt Express* 2008; 16: 16284–16293.
117. Faber C, Scherfig E, Prause JU & Sørensen KE. Corneal thickness in pigs measured by ultrasound pachymetry *in vivo*. *Scand J Lab Anim Sci* 2008; 35: 39–43.
118. Yang J, Zeng Y, Huang K & Li Z. Biomechanical properties of human and porcine cornea. *Chin J Biomed Eng* 2000; 20: 166–169.
119. Elsheikh A, Alhasso D & Rama P. Biomechanical properties of human and porcine corneas. *Exp Eye Res* 2008; 86: 783–790.
120. Bozkir G, Bozkir M, Dogan H, Aycan K & Güler B. Measurements of axial length and radius of corneal curvature in the rabbit eye. *Acta Med Okayama* 1997; 51: 9–11.
121. Hammer A, Kling S, Boldi M-O *et al.* Establishing corneal cross-linking with riboflavin and UV-A in the mouse cornea *in vivo*: biomechanical analysis. *Invest Ophthalmol Vis Sci* 2015; 56: 6581–6590.
122. Pandolfi A & Holzapfel GA. Three-dimensional modeling and computational analysis of the human cornea considering distributed collagen fibril orientations. *J Biomech Eng* 2008; 130: 1–12.
123. Roy AS, Rocha KM, Randleman JB, Stulting RD & Dupps WJ. Inverse computational analysis of *in vivo* corneal elastic modulus change after collagen crosslinking for keratoconus. *Exp Eye Res* 2013; 113: 92–104.
124. Pinsky PM, van der Heide D & Chernyak D. Computational modeling of mechanical anisotropy in the cornea and sclera. *J Cataract Refr Surg* 2005; 31: 136–145.
125. Elsheikh A & Wang D. Numerical modelling of corneal biomechanical behaviour. *Comput Method Biomec* 2007; 10: 85–95.
126. Pandolfi A & Manganiello F. A model for the human cornea: constitutive formulation and numerical analysis. *Biomech Model Mechan* 2006; 5: 237–246.
127. Roy AS & Dupps WJ. Patient-specific computational modeling of keratoconus progression and differential responses to collagen cross-linking. *Invest Ophthalmol Vis Sci* 2011; 52: 9174–9187.
128. Seven I, Roy AS & Dupps WJ. Patterned corneal collagen crosslinking for astigmatism: computational modeling study. *J Cataract Refr Surg* 2014; 40: 943–953.
129. Pinsky PM & Datye DV. A microstructurally-based finite element model of the incised human cornea. *J Biomech* 1991; 24: 907–922.
130. Alastrué V, Calvo B, Pena E & Doblaré M. Biomechanical modeling of refractive corneal surgery. *J Biomech Eng* 2006; 128: 150–160.
131. Pandolfi A, Fotia G & Manganiello F. Finite element simulations of laser refractive corneal surgery. *Eng Comput* 2009; 25: 15–24.
132. Roy AS & Dupps WJ. Patient-specific modeling of corneal refractive surgery outcomes and inverse estimation of elastic property changes. *J Biomech Eng* 2011; 133: 011002.
133. Roy AS, Dupps WJ & Roberts CJ. Comparison of biomechanical effects of small-incision lenticule extraction and laser *in situ* keratomileusis: finite-element analysis. *J Cataract Refr Surg* 2014; 40: 971–980.
134. Reinstein DZ, Archer TJ & Randleman JB. Mathematical model to compare the relative tensile strength of the cornea after PRK, LASIK, and small incision lenticule extraction. *J Refract Surg* 2013; 29: 454–460.
135. Roy AS & Dupps WJ. Effects of altered corneal stiffness on native and postoperative LASIK corneal biomechanical behavior: a whole-eye finite element analysis. *J Refract Surg* 2009; 25: 875–887.
136. Fleming JF, Wan WL & Schanzlin DJ. The theory of corneal curvature change with the intrastromal corneal ring. *Eye Contact Lens* 1989; 15: 146–150.

137. Kling S & Marcos S. Finite-element modeling of intrastromal ring segment implantation into a hyperelastic cornea. *Invest Ophthalmol Vis Sci* 2013; 54: 881–889.
138. Pinsky P, Datye D & Silvestrini T, editors. Numerical simulation of topographical alterations in the cornea after ICR (R)(intrastromal corneal ring). *Invest Ophthalmol Vis Sci* 1995; 36: S308.
139. Lago M, Rupérez M, Monserrat C *et al.* Patient-specific simulation of the intrastromal ring segment implantation in corneas with keratoconus. *J Mech Behav Biomed* 2015; 51: 260–268.

Sabine Kling is a postdoctoral researcher in the Ocular Cell Biology group at the University of Zurich, Switzerland, and investigates the relationship between corneal biomechanics and gene expression. She also develops models to optimise corneal cross-linking and refractive surgeries. In 2009, Kling graduated in Physical Engineering with honours from the University of Isny, Germany. She performed her pre-doctoral studies at the Optics Institute of the Spanish Council for Scientific Research in Madrid, where she investigated the measurement, modification and simulation of corneal biomechanics. In 2011, she earned her MSc and in 2014 her PhD degree in Vision Sciences, both with honours from the University of Valladolid, Spain. Kling's scientific work has been cited more than 396 times, she has a cumulative impact factor of 60, and an h-index of 10.

Farhad Hafezi is a Swiss eye surgeon and researcher. Hafezi holds professorships at the University of Geneva and University of Southern California, Los Angeles. He also serves as the chief medical officer of the ELZA Institute in Zurich, Switzerland, where he conducts his surgical activities. Hafezi is internationally recognized as a pioneer of corneal cross-linking (CXL) for treating keratoconus and a pacemaker in translating CXL principles to new applications like infections. In both 2014 and 2016, he was voted by his peers onto the "PowerList 100." This list comprises the 100 top most influential people in global ophthalmology. Clinically, Hafezi's expertise includes corneal diseases, dystrophies and degenerations as well as complication management related to refractive surgery. His research is dedicated to understanding corneal diseases with a special emphasis on ocular cell biology. Hafezi's scientific work has so far been cited more than 5300 times, he has a cumulative impact factor of 460, and an h-index of 38.

